The wing of the enhancer-binding domain of Mu phage transposase is flexible and is essential for efficient transposition

(helix–turn–helix/mutagenesis/NMR/heteronuclear relaxation)

ROBERT T. CLUBB*, MICHIYO MIZUUCHI†, JEFFREY R. HUTH*, JAMES G. OMICHINSKI*, HARRI SAVILAHTI†, KIYOSHI MIZUUCHI†, G. MARIUS CLORE*‡, AND ANGELA M. GRONENBORN*‡

Laboratories of *Chemical Physics and †Molecular Biology, Building 5, National Institute of Diabetes and Digestive and Kidney Diseases, National Institutes of Health, Bethesda, MD 20892-0520

ABSTRACT   A tetramer of the Mu transposase (MuA) pairs the recombination sites, cleaves the donor DNA, and joins these ends to a target DNA by strand transfer. Juxtaposition of the recombination sites is accomplished by the assembly of a stable synaptic complex of MuA protein and Mu DNA. This initial critical step is facilitated by the transient binding of the N-terminal domain of MuA to an enhancer DNA element within the Mu genome (called the internal activation sequence, IAS). Recently we solved the three-dimensional solution structure of the enhancer-binding domain of Mu phage transposase (residues 1–76, MuA⁷⁶) and proposed a model for its interaction with the IAS element. Site-directed mutagenesis coupled with an *in vitro* transposition assay has been used to assess the validity of the model. We have identified five residues on the surface of MuA that are crucial for stable synaptic complex formation but dispensable for subsequent events in transposition. These mutations are located in the loop (wing) structure and recognition helix of the MuA⁷⁶ domain of the transposase and do not seriously perturb the structure of the domain. Furthermore, in order to understand the dynamic behavior of the MuA⁷⁶ domain prior to stable synaptic complex formation, we have measured heteronuclear ^{15}N relaxation rates for the unbound MuA⁷⁶ domain. In the DNA free state the backbone atoms of the helix–turn–helix motif are generally immobilized whereas the residues in the wing are highly flexible on the pico- to nanosecond time scale. Together these studies define the surface of MuA required for enhancement of transposition *in vitro* and suggest that a flexible loop in the MuA protein required for DNA recognition may become structurally ordered only upon DNA binding.

Transposition is a genetic recombination reaction that moves a mobile DNA element, known as a transposon, from one site to another in the DNA of the host organism. The reaction involves two chemical steps: (*i*) endonucleolytic cleavage of the phosphodiester bond between the transposon DNA and the host DNA and (*ii*) strand transfer, which involves the covalent linkage of the 3' ends of the donor DNA to the new host DNA target site (1). Retroviruses and retrotransposons use a similar mechanism to integrate reverse-transcribed copies of their genomes into the DNA of the host cell. Typically, a single protein, the integrase or transposase, is responsible for both DNA cleavage and strand transfer reactions. The largest and most efficient transposon known is the Mu phage genome, which uses the phage-encoded transposase (MuA protein) to pair the ends of the phage DNA, cleave the termini, and promote strand transfer (2–4).

Transposition of the Mu genome occurs in the context of several higher-order protein–DNA complexes and is initiated by the coordinated assembly of a tetramer of transposase onto the Mu DNA (2, 5, 6). This nucleoprotein intermediate, called the stable synaptic complex, contains the left and right ends of the Mu DNA held in close proximity by a tetramer of MuA. Formation of the stable synaptic complex requires two distinct cis-acting DNA sequences on the Mu genome. The MuA protein initially binds to six similar DNA sequences, three at each end of the Mu genome (sites L1–L3 on the left end and sites R1–R3 on the right end). A second distinct DNA sequence located about 1 kb from the left end, called the internal activation sequence (the IAS, or transpositional enhancer), is then transiently occupied by the MuA protein, facilitating the assembly of the stable synaptic complex. This protein–DNA structural rearrangement is assisted by the host-encoded DNA-bending proteins HU and IHF and provides an important topological filter, ensuring that only suitably arranged Mu DNA will be transposed. An additional level of regulation is achieved by the action of the Mu repressor. DNA sequence identity between the IAS element and the Mu operator site and primary sequence homology between the N-termini of the repressor and transposase proteins may allow the Mu repressor to prevent spurious transposition events during viral latency.

The N-terminal domain of MuA (35 kDa) binds DNA sequence-specifically and is essential for stable synaptic complex formation. It is constructed of two separate DNA-binding domains, comprising residues 1–76 and 77–247, which bind to the IAS element and the ends of the phage genome, respectively (7, 8). Recently, we solved the three-dimensional solution structure of the N-terminal IAS DNA-binding domain of Mu phage transposase (residues 1–76, MuA⁷⁶) and proposed a model for its interaction with DNA (9).

Here we present the results of both site-directed mutagenesis and heteronuclear ^{15}N relaxation experiments designed to elucidate the molecular basis of MuA⁷⁶ domain function. Several residues at the putative transposase/IAS DNA interface in our model of the complex (9) were targeted for mutagenesis and the effects of these amino acid changes were assessed in an *in vitro* transposition assay. The results of the assay are entirely consistent with the model of the complex and provide direct evidence that both a loop structure and DNA recognition helix in the MuA⁷⁶ domain of transposase are crucial for stable synaptic complex formation. Further, this essential loop element exhibits substantial mobility in the absence of DNA as evidenced by heteronuclear relaxation measurements. The results of both biochemical and biophysical studies provide a detailed picture of the function of the MuA⁷⁶ domain during transposition.

MATERIALS AND METHODS

MuA⁷⁶ Heteronuclear Relaxation Studies. The N-terminal IAS DNA-binding domain of Mu phage transposase [residues

Abbreviations: DMSO, dimethyl sulfoxide; IAS, internal activation sequence; NOE, nuclear Overhauser effect.
‡To whom reprint requests should be addressed.

1–76 with a Cys-to-Leu substitution at position 10 (C10L), MuA[76]] used for NMR studies was uniformly (>95%) ^{15}N-labeled and purified as described (9). Data were collected on a 1.0 mM protein sample in 90% H_2O/10% ^2H_2O/250 mM NaCl, pH 5.8 at 20°C, with a Bruker (Billerica, MA) model AMX600 spectrometer.

The ^{15}N relaxation data were obtained as described (10–15). [15]N T_2 values were obtained by using delays of 8, 16, 40, 48, 64, 88, 120, 160 and 208 ms. [15]N T_1 values were measured by using delays of 52, 244, 372, 532, 700, 852, and 1124 ms. The decays of the cross-peak intensities with time were fit to a single exponential by nonlinear least-squares methods. Fitting errors of the T_1 and T_2 values were typically less than 3–4%. The errors in the nuclear Overhause effect (NOE) measurements were on the order of ±0.1. Model-free parameters were determined by nonlinear least-squares minimization of the sum of the error-weighted residuals between the calculated and experimental data, using the Levenburg–Marquardt algorithm (16). Precision estimates of the extracted model-free parameters were obtained by Monte Carlo simulation (17).

Site-Directed Mutagenesis. Mutagenesis was accomplished by the overlapping template method (18). The original template was derived from plasmid pMK609, which carried the coding sequence for the full-length MuA protein with the C10L mutation cloned between the *Nde* I and *Bam*HI sites of a pET3c vector. Suitable primers were purchased from Bio-Serve Biotechnologies (Laurel, MD). The reading frames of the mutated full-length MuA proteins (residues 1–663) were cloned between the *Nde* I and *Bam*HI sites of the T7 RNA polymerase expression vector pET3c (Novagen) and overexpressed in NovaBlue(DE3) bacterial cells (Novagen). The presence of each mutation in the protein expression vector was confirmed by sequencing the DNA coding for residues 1–76 of MuA. Reading frames corresponding to residues 1–76 of MuA were generated by using the mutated full-length constructs as templates along with suitable primers. Each truncated reading frame was then cloned between the *Nde* I and *Bam*HI sites of the pET3c vector and overexpressed in BL21(DE3) bacterial cells.

Transposition Reactions. Standard reaction conditions were used (19, 20). Reaction mixtures contained 25 mM Tris·HCl (pH 8), 156 mM NaCl, 10 mM $MgCl_2$, 2 mM ATP, 1 mM dithiothreitol, 15% (vol/vol) glycerol, bovine serum albumin at 25 μg/ml, donor DNA at 10 μg/ml, and φX174 replicative form (RF) DNA at 10 μg/ml. The reaction volume was 25 μl and contained the following protein levels: MuB, 6.5 pmol;

HU, 3.0 pmol; and MuA variants, 3.7 μg/ml. When indicated dimethyl sulfoxide (DMSO) was added to 15% (vol/vol). Proteins were added as 1-μl aliquots to the reaction mixture after the appropriate dilution of a stock solution (20). Preparation of buffers, proteins, and donor/target DNA plasmids was as described (8, 20). All reaction mixtures were incubated at 30°C for 1 hr, stopped by the addition of 0.2 vol of stop solution (0.1% bromophenol blue/2.5% SDS/50 mM EDTA/ 25% Ficoll) and analyzed by gel electrophoresis (19, 20).

RESULTS

Side Chains in the Winged Helix–Turn–Helix Motif Are Critical for IAS Recognition. Site-specific mutations in the enhancer-binding domain of Mu transposase were introduced to investigate their effects on transposition. Mutation sites were selected on the basis of a model of the MuA[76]–DNA complex proposed on the basis of NMR data (9), which predicted that a helix–turn–helix DNA-binding motif and a structurally disordered loop in the MuA[76] domain of MuA function to recognize the IAS DNA binding site.

Seven modifications to the structure of the full-length MuA protein were introduced and tested with an *in vitro* transposition assay. The following MuA constructs were investigated: (*i*) a single point mutant, C10L, to place the exact sequence used in our NMR studies of the MuA[76] domain fragment in the context of the full-length protein; (*ii*) five double mutants which contain the C10L mutation and an additional alteration in the putative protein DNA interface, C10L/K18E, C10L/ A21K, C10L/Y25E, C10L/K29E, and C10L/K44E; and (*iii*) a truncated MuA protein which lacks the enhancer-binding domain, MuA(Δ1–76). The altered proteins were overexpressed in *Escherichia coli*, purified to >90% homogeneity, and assayed to determine their ability to support strand transfer in an *in vitro* reaction (Fig. 1). Under standard reaction conditions with mini-Mu donor DNA (pMK586) in supercoiled form, and φX174 RF target DNA, wild-type MuA protein can efficiently carry out the DNA strand transfer reaction in the presence of MuB and HU proteins (Fig. 1, lane 3). Consistent with previous studies, the enhancer-binding domain of MuA is essential for efficient transposition (8). Removal of this domain in the MuA(Δ1–76) protein results in failure to generate strand transfer products under standard reaction conditions (Fig. 1, lane 4). Double mutants of MuA that contain alterations in the putative protein/DNA interface and at position 10 (C10L) exhibit a phenotype similar to that
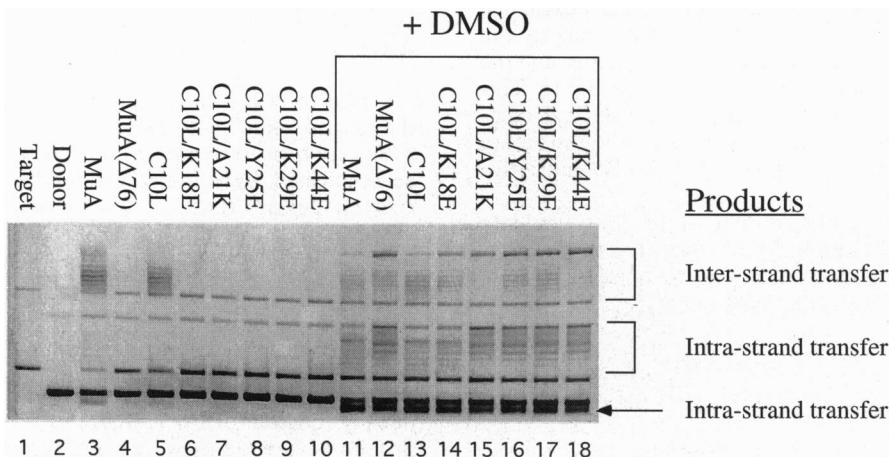

FIG. 1.   Agarose gel showing the results of the *in vitro* assay of six site-specific mutants of MuA transposase. The gel positions of the expected products of the reaction are indicated on the right. Initial reactants are shown in lanes 1 and 2 (target and donor DNA, respectively). Lanes 3 and 4 correspond to wild-type transposase (MuA) and residues 77–663 of transposase (MuAΔ76), respectively. Lanes 5–10 correspond to six site-specific mutants of MuA: C10L, C10L/K18E, C10L/A21K, C10L/Y25E, C10L/K29E and C10L/K44E, respectively. Lanes 11–18 are identical to lanes 3–10 but the reactions were performed in the presence of DMSO.

of the MuA(Δ1–76) protein and are unable to promote strand transfer (Fig. 1, lanes 6–10). The inability to promote strand transfer in the double mutants of MuA can be attributed to the surface mutations rather than the C10L mutation, since the single C10L mutant behaves like the wild type (Fig. 1, lane 5).

Mutants Are Unable to Assemble into a Stable Synaptic Complex but Are Active in Subsequent Cleavage and Transfer Events. Variants of MuA were tested for their ability to form stable nucleoprotein intermediates. The transposition reaction was performed as described above, except that pBR322 was used as the target DNA and the reaction products were visualized with nondenaturing gel electrophoresis (2). Under these conditions only wild-type MuA and MuA with the single C10L mutation were able to form stable protein–DNA intermediates. MuA proteins that lacked the enhancer-binding domain or that contained alterations in the winged helix–turn–helix domain were unable to form stable complexes on the phage DNA (data not shown). The surface mutants therefore exhibit a distinct phenotype as compared to the recently identified active-site mutants of MuA, which are capable of forming stable synaptic complexes (21).

To investigate whether variants of MuA retained the ability to perform subsequent cleavage and strand transfer reactions, the assay was repeated in the presence of DMSO. This condition eliminates the stringent requirement for the enhancer element as well as DNA supercoiling (8). As shown in Fig. 1, lanes 11–18, all forms of the MuA protein are active under these conditions, indicating that steps subsequent to the formation of the stable synaptic complex are unaffected by any of the changes introduced into the MuA[76] domain.

The DNA-Binding Loop Is Flexible. [15]N relaxation data were collected on the free MuA[76] domain to characterize the backbone mobility of this fragment. Spectra of the MuA[76] domain of transposase were assigned by using previously determined resonance assignments (9). The quality of the spectra allowed the relaxation behavior of 64 of 72 non-proline residues to be monitored. A summary of the [15]N T_1, T_2 and NOE data plotted as a function of residue number is shown in Fig. 2 *A* and *B*. In general, the data indicate that the majority of residues in MuA[76] exhibit uniform backbone mobility, with increased mobility between residues Ala[38] and Ile[46], comprising the wing region, and at the N and C termini.

The overall correlation time, determined from [15]N T_1/T_2 ratios by using the criteria described (10, 13) is 7.53 ± 0.06 ns. The ^{15}N NOE, T_1, and T_2 data for each residue were fit simultaneously to various forms of model-free spectral density function (11, 22, 23) in the presence or absence of an additional term ($\pi\Delta ex$) to account for the effects of chemical-exchange line broadening on T_2 (11). In the model-free analysis the overall motion of the protein is assumed to be isotropic and the internal motions independent of the overall tumbling. This approximation is reasonable, since the three principal components of the inertial tensor for the average solution structure of the MuA[76] domain are in a ratio of 1.00:1.76:1.45, indicative of a globular structure.

The spectral density functions used to fit the relaxation data differ in the degree of complexity assumed for the internal motions. Three models, containing one to three adjustable parameters, were used to fit the data:

$$J(\omega_i) = S^2\tau_r/(1 + \omega^2\tau_r^2), \qquad [1]$$

$$J(\omega_i) = S_2^\pi/(1 + \omega^2\tau_r^2) + (1 - S^2)\tau_e'/(1 + \omega^2\tau_e'^2), \qquad [2]$$

$$J(\omega_i) = S^2\tau_r/(1 + \omega^2\tau_r^2) + S_f^2(1 - S_s^2)\tau_s'/(1 + \omega^2\tau_s'^2), \qquad [3]$$

where S^2 is the generalized overall order parameter (22); τ_e is the internal correlation time [with $\tau_e' = \tau_r\tau_e/(\tau_r + \tau_e)$] (22); τ_s is the internal correlation time for the slow motions (with $\tau_s' = $
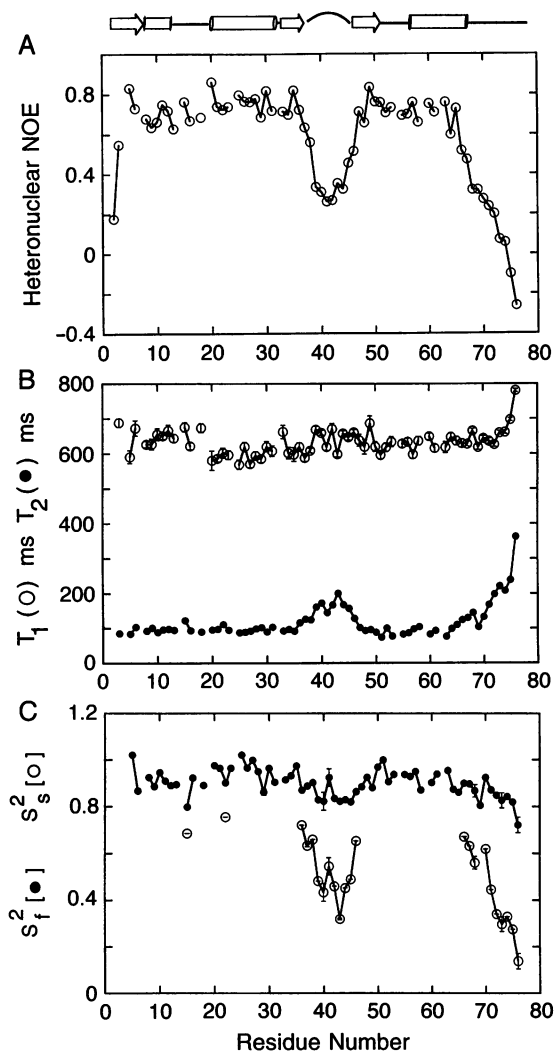

FIG. 2.   Graphical representation as a function of residue number of the backbone ^{15}N relaxation data at 600 MHz and the results of their analysis for MuA[76] at 20°C. (*A*) [15]N–[1]H NOEs. (*B*) [15]N T_1 (○) and [15]N T_2 (●) relaxation data at 600 MHz. (*C*) The fast S_f^2 (●) and slow S_s^2 (○) generalized motion order parameters. [For residues that were fit to the conventional Lipari and Szabo (22) spectral density function (either Eq. **1** or Eq. **2**), $S_f^2 = S^2$]. Fitting errors in the experimental T_1 and T_2 values and the standard deviations of the various calculated parameters are represented by vertical bars. The errors in the experimental [1]H–[15]N NOEs are on the order of ±0.1. The locations of the β-strands and α-helices are indicated above *A*.

$\tau_r\tau_s/(\tau_r + \tau_s)$ (23); and S_f^2 and S_s^2 are the order parameters for the fast and slow motions (23), respectively, with $S^2 = S_f^2 S_s^2$.

Selection of the appropriate spectral density function was accomplished by initially fitting the data to the simplest spectral density function and employing more complicated models only as required to fit the relaxation data. The experimental data of a residue were considered to be adequately represented by a particular spectral density function if the T_1 and T_2 data were reproduced to within 5% and the NOE data to within ±0.1 of their experimentally determined values.

The data for 12 of the 64 measurable backbone amide groups could be accounted for by the model-free spectral density function of Eq **1**, where τ_e is assumed to be <20 ps. Sixteen of 65 residues were reproduced with Eq. **2**, and the τ_e values of these residues ranged from 5.5 ps to 1 ns. Twenty-five of 49 residues were fit with Eq. **3** and had slow correlation times that ranged from 0.7 to 2.7 ns. Six residues (Lys[18], Asn[51], Leu[53], Val[55], Glu[56], and Ala[60]) are likely to exhibit a small amount of chemical exchange line broadening, since they have T_1/T_2

ratios that are more than one standard deviation above the mean T_1/T_2 ratio of residues with NOE values > 0.6. These residues were fit with Eq. **1** together with an additional term to account for the effect of chemical exchange line broadening on T_2 (11). The magnitudes of these processes are relatively small, with a maximum increase in the ^{15}N linewidth of 0.8 ± 0.1 Hz for Leu[53]. The data for all residues were adequately reproduced, with the exception of four residues. The T_1 and T_2 data for residues Lys[18], Leu[10], and Val[55] were reproduced, while their NOE data were consistently underestimated. All the relaxation data for Glu[2] were inadequately reproduced by Eqs. **1–3**, suggesting that this residue undergoes very complicated motions. The results of the data analysis are summarized in Fig. 2C, which shows a plot of the fast and slow order parameters as a function of residue number.

DISCUSSION

To understand the complex process of DNA transposition, we have conducted site-directed mutagenesis and NMR spectroscopic studies of the enhancer-binding domain of MuA. These studies define the surface of MuA required for enhancement of transposition *in vitro* and provide valuable insights into the dynamic behavior of the enhancer-binding domain prior to IAS DNA recognition.

Exploiting knowledge of the three-dimensional structure of the enhancer-binding domain (9), we have rationally probed the surface of full-length MuA protein to identify regions that are essential for recognition of the IAS DNA element. The solution structure of the MuA[76] domain of MuA (Fig. 3) begins with strand B1 (Trp[4]–Ser[6]), which pairs with strand B2 (Trp[32]–Arg[35]) before ascending into a short helix (H1, Lys[8]–Asn[12]). The sequence then forms an 8-residue turn (T) that connects H1 to helix H2 (Ser[20]–Lys[29]). The structure of the H1–T–H2 segment is similar to the helix–turn–helix DNA-binding motif used by a variety of proteins (25). Strand B2 follows the helix–turn–helix motif and pairs with strand B3 (Ala[45]–Asn[49]). A large partially disordered loop comprising residues Thr[36]–Lys[44] connects strands B2 and B3 and protrudes from the globular core. The remainder of the protein consists of strand B3 and the C-terminal helix H3 (Val[55]–Gln[65]), which pack against B1 and H1 to seal the protein core. The relative positioning of a helix–turn–helix motif and a loop between strands B2 and B3 in MuA[76] (Fig. 3) are structurally analogous
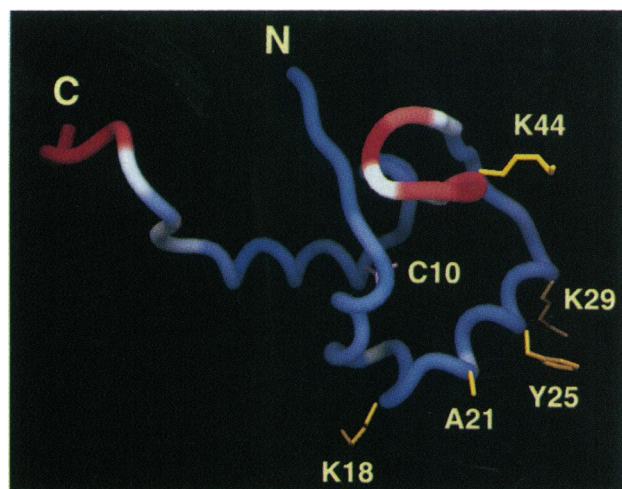

FIG. 3. The backbone structure of the MuA[76] domain color-coded for the generalized order parameter S^2 varying from red (high mobility, $S^2 = 0.3$) to white (intermediate mobility, $S^2 = 0.6$) to blue (low mobility, $S^2 = 1.0$). Side chains of residues mutated in this study are displayed. The coordinates are from ref. 9 and the figure was generated with the program GRASP (24).

to the HNF-3γ/fork head motif structure (26). In the cocrystal structure, the HNF-3γ/fork head motif interacts with DNA by using a helix–turn–helix motif and two wings, a loop between strands B2 and B3, called W1, and the C terminus, called W2 (26). In the MuA[76]–IAS DNA model (9) the recognition helix (H2) of MuA[76] fits into the major groove and the loop connecting strands B2 and B3 contacts the DNA. Potential hydrophobic contacts are made by the side chains of residues Ala[21], Ile[24], Tyr[25], and Ile[46]. Residues Lys[8], Lys[15], Ser[20], Lys[28], Lys[29], Asn[34], and Lys[44] may form hydrogen bonds or electrostatic contacts with the DNA (figure 6 in ref. 9).

We have used site-directed mutagenesis coupled with an *in vitro* transposition assay to assess the validity of the model. Two potential hydrophobic contacts involving Ala[21] and Tyr[25] have been removed and three potential hydrogen-bond/electrostatic interactions involving Lys[18], Lys[29], and Lys[44] have been altered in the full-length MuA protein (Fig. 3). We postulate that these alterations will prevent IAS binding and will therefore inhibit the ability of MuA to perform strand transfer. The transposition assay provides an indirect measure of the affinity of the MuA[76] domain of full length transposase for the IAS element, since the function of the enhancer-binding domain (residues 1–76) is intimately linked to IAS DNA binding (7, 8). As shown in Fig. 1 (lane 3) wild-type MuA protein is able to covalently link suitable donor and target DNA in the presence of the appropriate accessory factors. However, when residues 1–76 from the MuA protein are deleted (MuAΔ76), strand transfer does not occur in the absence of DMSO (Fig. 1, lane 4). The MuA[76]–IAS DNA model is based on the structure of a MuA[76] domain fragment with a Cys-to-Leu mutation at position 10 (C10L) (9). To control for the effects of this mutation on transposition, we created a single C10L mutant of intact MuA protein and tested its ability to perform strand transfer. The C10L mutation has no obvious effect on strand transfer in the presence or absence of DMSO (Fig. 1, compare lane 3 with lane 5 and lane 11 with lane 13). On the other hand, all of the surface mutants that contain amino acid changes in the recognition helix H2 (A21K, Y25E, K29E), the preceding turn (K18E), or the wing (K44E) in addition to the C10L mutation are unable to perform strand transfer *in vitro* (Fig. 1, lanes 6–10). In fact, the phenotypes of these double mutants are indistinguishable from that of MuA protein that lacks the MuA[76] domain altogether.

The above surface mutations of the MuA protein prevent the formation of stable synaptic complexes but do not seriously alter the structure of the MuA[76] domain. The presence of DMSO in the transposition assay eliminates the stringent requirement for the enhancer element as well as DNA supercoiling and allows subsequent transposition steps to be tested. As shown in Fig 1 (lanes 11–18), all MuA constructs are active in the presence of DMSO, indicating that strand cleavage and transfer reactions are unaffected in these proteins. Furthermore, reaction products analyzed by nondenaturing gel electrophoresis indicate that only the wild-type MuA and the C10L mutant assemble into stable synaptic complexes. Failure of the five double mutants to properly assemble onto the donor plasmid is not caused by disruption of the structure of the MuA[76] domain, since polypeptides comprising residues 1–76 with the C10L mutation and all of the five surface mutations remain folded (as judged by ^1H–^{15}N correlation spectra of partially purified extracts containing overexpressed MuA[76] double mutants). This leads us to conclude that the double mutants are unable to properly interact with the IAS element on the donor DNA.

The MuA[76] domain exhibits significant mobility when not bound to its cognate DNA sequence, as evidenced by backbone relaxation measurements. The results of the relaxation data analysis can best be interpreted by mapping them onto the solution structure of MuA[76]. Fig. 3 displays the variation of the generalized order parameter (S^2) as a color gradient from red

(high mobility) to blue (low mobility) on a ribbon diagram of the three-dimensional structure. Clearly, residues in the disordered loop (wing) between strands B2 and B3 and at the C terminus are highly mobile. The dynamic behavior of the remainder of the protein is uniform and shows a high degree of motional restriction. These results indicate that in the DNA free state the backbone atoms of the helix–turn–helix motif are generally immobilized whereas the residues in the wing are highly flexible on the pico- to nanosecond time scale. Interestingly, residues in the wing do not exhibit shortened ^{15}N T_2 values, indicating that this region of the protein does not jump between magnetically inequivalent conformations on a microsecond time scale. The MuA^{76} domain may therefore use very rapid polypeptide fluctuations of the wing motif to facilitate dynamic transient recognition of the IAS element during transposition.

1. Mizuuchi, K. (1992) *Annu. Rev. Biochem.* **61,** 1011–1051.
2. Mizuuchi, M., Baker, T. A. & Mizuuchi, K. (1992) *Cell* **70,** 303–311.
3. Craigie, R. & Mizuuchi, K. (1987) *Cell* **51,** 493–501.
4. Surette, M. G., Buch, S. J. & Chaconas, G. (1987) *Cell* **49,** 253–262.
5. Baker, T. A. & Mizuuchi, K. (1992) *Genes Dev.* **6,** 2221–2232.
6. Surette, M. G. & Chaconas, G. (1992) *Cell* **68,** 1101–1108.
7. Leung, P. C., Teplow, D. B. & Harshey, R. M. (1989) *Nature (London)* **338,** 656–658.
8. Mizuuchi, M. & Mizuuchi, K. (1989) *Cell* **58,** 399–408.
9. Clubb, R. T., Omichinski, J. G., Savilahti, H., Mizuuchi, K., Gronenborn, A. M. & Clore, G. M. (1994) *Structure* **2,** 1041–1048.
10. Kay, L. E., Torchia, D. A. & Bax, A. (1989) *Biochemistry* **28,** 8972–8979.
11. Clore, G. M., Driscoll, P. C., Wingfield, P. T. & Gronenborn, A. M. (1990) *Biochemistry* **29,** 7387–7401.
12. Grasberger, B. L., Gronenborn, A. M. & Clore, G. M. (1993) *J. Mol. Biol.* **230,** 364–372.
13. Barchi, J. J., Grasberger, B. L., Gronenborn, A. M. & Clore, G. M. (1994) *Protein Sci.* **3,** 15–21.
14. Clubb, R. T., Omichinski, J. G., Sakaguchi, K., Appella, E., Gronenborn, A. M. & Clore, G. M. (1995) *Protein Sci.* **4,** 855–862.
15. Grzesiek, S. & Bax, A. (1993) *J. Am. Chem. Soc.* **115,** 12593–12594.
16. Press, W. H., Flannery, B. P., Teukolsky, S. A. & Vetterling, W. T. (1986) *Numerical Recipes in C* (Cambridge Univ. Press, Cambridge, U.K.).
17. Kamath, U. & Shriver, J. W. (1989) *J. Biol. Chem.* **264,** 5586–5592.
18. Ausubel, F. M., Brent, R., Kingston, R. E., Moore, D. D., Seidman, J. G., Smith, J. A. & Struhl, K. (1995) *Current Protocols in Molecular Biology* (Wiley, New York), Vol. 1, pp. 8.5.7–8.5.9.
19. Craigie, R. & Mizuuchi, K. (1985) *Cell* **41,** 867–876.
20. Baker, T. A., Mizuuchi, M., Savilahti, H. & Mizuuchi, K. (1994) *Cell* **74,** 723–733.
21. Baker, T. A. & Luo, L. (1994) *Proc. Natl. Acad. Sci. USA* **91,** 6654–6658.
22. Lipari, G. & Szabo, A. (1982) *J. Am. Chem. Soc.* **104,** 4546–4559.
23. Clore, G. M., Szabo, A., Bax, A., Kay, L. E., Driscoll, P. C. & Gronenborn, A. M. (1990) *J. Am. Chem. Soc.* **112,** 4989–4991.
24. Nicholls, A. J. (1993) GRASP *Manual* (Columbia Univ. Press, New York).
25. Harrison, S. C. & Aggarwal, A. K. (1990) *Annu. Rev. Biochem.* **59,** 933–969.
26. Clarke, K. L., Halay, E. D., Lai, E. & Burley, S. K. (1991) *Nature (London)* **364,** 412–420.